Published in final edited form as:
J Immunol. 2012 October 15; 189(8): 3894–3904. doi:10.4049/jimmunol.1200783.

miRNAs control the maintenance of thymic epithelia and their competence for T lineage commitment and thymocyte selection

Saulius Zuklys[*,1], **Carlos E. Mayer**[*,1], **Saule Zhanybekova**[*], **Heather E. Stefanski**[†], **Gretel Nusspaumer**[*], **Jason Gill**[*], **Thomas Barthlott**[*], **Stephane Chappaz**[‡], **Takeshi Nitta**[§], **James Dooley**[¶], **Ruben Nogales-Cadenas**[||], **Yousuke Takahama**[§], **Daniela Finke**[‡], **Adrian Liston**[¶], **Bruce R. Blazar**[†], **Alberto Pascual-Montano**[||], and **Georg A. Holländer**[*,#]

[*]Pediatric Immunology, Department of Biomedicine, University of Basel and The Basel University Children's Hospital, Basel, Switzerland [†]Cancer Center and Department of Pediatrics, Division of Blood and Marrow Transplantation, University of Minnesota, Minneapolis, USA [‡]Developmental Immunology, Department of Biomedicine, University of Basel, and The Basel University Children's Hospital, Basel, Switzerland [§]Division of Experimental Immunology, University of Tokushima, Japan [¶]Autoimmune Genetics Laboratory, VIB and University of Leuven, Leuven, Belgium [||]Functional Bioinformatics Group, National Center for Biotechnology-CSIC, Madrid, Spain [#]Developmental Immunology, Department of Paediatrics, University of Oxford, Oxford, United Kingdom

Abstract

Thymic epithelial cells provide unique cues for the life-long selection and differentiation of a repertoire of functionally diverse T cells. Rendered miRNA deficient, these stromal cells in the mouse lose their capacity to instruct the commitment of haematopoietic precursors to a T cell fate, to effect thymocyte positive selection and to achieve promiscuous gene expression required for central tolerance induction. Over time, the microenvironment created by miRNA-deficient thymic epithelia assumes the cellular composition and structure of peripheral lymphoid tissue where thympoiesis fails to be supported. These findings emphasize a global role for miRNA in the maintenance and function of the thymic epithelial cell scaffold and establish a novel mechanism how these cells control peripheral tissue antigen expression to prompt central immunological tolerance.

Introduction

The thymus provides a unique stromal microenvironment that instructs the differentiation of blood-borne precursors to functionally mature T lymphocytes proficient to effect an immune response against microbial pathogens whilst unable to elicit an autoimmune reaction (1). The major structural components of the thymus are thymic epithelial cells (TEC) that can further be classified as cortical (c) or medullary (m) TEC subpopulations based on distinct structural, antigenic and functional features (2,3). The molecular programs that control TEC growth, differentiation, and maintenance are, however, only incompletely characterized.

Correspondence should be addressed to: Georg A. Holländer, Laboratory of Pediatric Immunology, Center for Biomedicine, University of Basel, Mattenstrasse 28, 4058 Basel, Switzerland. Phone: +41-61-695-3069, Fax: +41-61-695-3070, georg-a.hollaender@unibas.ch.
[1]Contributed equally to the work

Disclosure
The authors declare no competing financial interests.

The most immature T cell precursors differentiate within the thymic cortex where they acquire the expression of both CD4 and CD8 (double positive, DP stage of development) and eventually express the complete αβ T cell antigen receptor (TCR) (4). As their antigen specificity is randomly generated, DP thymocytes are subjected to a selection process aimed at testing their suitability for a given individual. Known as positive selection, thymocytes with a TCR that recognizes self-peptide/MHC complexes on cTEC with sufficient affinity will continue their intrathymic maturation and migrate to the medulla. There, thymocytes are exposed to a negative selection. This process purges TCR-bearing cells with an affinity for self-peptide/MHC complexes above a critical threshold and thus prevents self-antigen recognition by T cells of extra thymic tissue which may elicit autoimmunity.

Micro RNA (miRNA) represent an essential class of small (19–25 nucleotides, nt), non-coding RNAs indispensible for biological processes including cell fate determination, self-renewal, differentiation, proliferation, apoptosis and cellular homeostasis (5). Primary miRNA transcripts are processed by nuclear RNAse III enzyme Drosha and its co-factor DGCR8 to intermediate miRNAs which are exported to the cytoplasm. There, a second RNAse III enzyme, designated Dicer, catalyzes the formation of miRNA duplexes. These short sequences are integrated into the RNA-induced silencing complexes (RISC) and control protein synthesis by interacting with target messenger RNA either repressing translation or mediating RNA cleavage and degradation (6). A single miRNA species may regulate the expression of hundreds of proteins, though the repression is usually mild and frequently the result of both downregulation of mRNA levels and inhibition of translation (7–9). Cell- and tissue-specific miRNA expression patterns have been identified, suggesting unique biological roles for specific miRNA. However, the precise functions for almost all of the at least 1055 mouse miRNA remain to be experimentally verified (10). To judge the global role of miRNA for the development, function and homeostasis of TEC, we generated mice with a TEC targeted Dicer deficiency.

Material and Methods

Mice

Mice were kept under specific pathogen free conditions and used according to federal and institutional regulations. For developmental staging, the day of the vaginal plug was designated as embryonic day (E) 0.5. C57BL/6 mice were obtained in-house from the Departmental breeding facility whereas nude (nu/nu) mice were obtained from a commercial vendor (Janvier, France). Mice were kept and handled according to Cantonal and Federal regulations and permissions.

Histology and immunofluorescence

Frozen thymus tissue sections (8μm) were fixed in gradient ethanol solutions and stained with Mayer's hematoxyline (Réactifs RAL) and eosin (J. T. Baker). For immunohistochemistry, acetone-fixed sections (8μm) were stained using antibodies specific for cytokeratin (CK) 5 (Covance), CK8 (Progen), CK14 (Covance), MTS10 (a gift from R. Boyd, Melbourne, Australia), ERTR7 (provided by W. vanEwijk, Utrecht, Netherlands), Psmb11 (MBL), Lyve1 (ReliaTech), CR1 (8C12, Becton-Dickinson), Aire (5H12, provided by S. Hamish, Adelaide, Australia), PNAd (MECA-79, Becton-Dickinson), and reactivity to lectin UEA-1 (Reactolab). Alexa-Fluor conjugated anti-IgG antibodies (Invitrogen) were used as secondary reagents. Images were acquired using a Zeiss LSM510.

Flow cytometry, cell sorting and intracytoplasmic staining

Haematopoietic cells from thymus and spleen were stained with Abs against CD3 (KT-3), CD4 (GK1.5, BioLegend), CD8 (53–67, eBioscience), CD19 (ID3), CD25 (PC61.5,

eBioscience), CD44 (IM7, eBioscience), CD62L (MEL-14, Becton-Dickinson), CD69 (H1.2F3, Becton-Dickinson), CD93 (aa4.1, eBioscience) and IgM (R33.24.12). For intracellular staining, cells were fixed and permeabilized using the Cytofix/Cytoperm Kit (Becton-Dickinson) and stained for Foxp3 expression (FJK-16s, eBioscience). For the analysis of TEC, thymic lobes were cut into small pieces, and then incubated at 37°C for 60 minutes in HBSS containing 2% (w/v) FCS (Perbio), 100μg/ml Collagenase/Dispase (Roche Diagnostics) and 40ng/ml DNaseI (Roche). TECs were enriched using AutoMACS (Miltenyi Biotec) and stained for the expression of EpCAM (G8.8, DSHB, University of Iowa), CD45 (30F11, eBioscience), MHCI (AF6-88.5, Biolegend), MHCII (AF6-120.1, BioLegend), Ly51 (6C3, BioLegend) Dll-4 (gift from Robson MacDonald, University of Lausanne) and UEA-1 (Reactolab). For intracellular staining, TECs were marked for cell surface molecules, fixed, permeabilized (Cytofix/Cytoperm, Becton-Dickinson) and stained with BrdU or Aire-specific antibodies. Flow cytometric analysis and cell sorting were performed (FACSAria) using FACSDiva (Becton-Dickinson) and FlowJo software (TreeStar).

MicroRNA detection and gene expression profiling

Total RNA was isolated from sorted cells with the miRNeasy Mini Kit (Qiagen). The QuantiMir RT Kit (System Biosciences) was utilized to analyze the expression of specific miRNA. cDNA was assessed by quantitative real-time PCR with SYBR Green (SensiMix, Bioline). Primer sequences are available upon request. Gapdh was used as an internal control for miRNA and mRNA analysis respectively. The mRNA expression profiles in TEC isolate from 2 week old Foxn1Cre::Dicer$^{fl/fl}$ and Dicer$^{fl/fl}$ mice were generated using the GeneChip Gene 1.0 ST Array System (Affymetrix). The array data were submitted to the ArrayExpress repository under accession E-MEXP-3303 (http://www.ebi.ac.uk/arrayexpress/experiments/E-MEXP-3303).

Bioinformatic and statistical analysis

Differential expression analysis for mRNA was carried out using Partek® application software (www.partek.com) and visualized with Integromics Biomarker Discovery for Tibco Spotfire® (www.integromics.com). The gene expression data were normalized using Affymetrix Robust Multi-Array Analysis (RMA) and differential expression was obtained by analysis of variance (Two-way ANOVA). P-value correction for multiple hypothesis was performed with Benjamini-Hochberg's false discovery rate (FDR) (11). Functional analyses of biological processes were determined by Genecodis determining the significantly enriched gene ontology terms in the list of gene targets (12,13).

BrdU analysis

Mice were injected intraperitoneally (i.p.) with 1mg BrdU in phosphate buffered saline and TECs were analyzed 4 hours later by flow cytometry (see above).

Bone marrow chimeric mice

Sub-lethally irradiated newborn Foxn1Cre::Dicer$^{fl/fl}$ and Dicer$^{fl/fl}$ mice were injected i.p. with OT1 transgenic fetal liver cells (2×10^6) from E13.5–14.5 old embryos. Successfully grafted animals (with an average chimerism of at least 30% for OT1) were analyzed 4 weeks later.

T-cell depletion

Two-week old mice were injected i.p. three times every three days with 200μg anti-CD4 (GK1.5), 100μg anti-CD8 (53–67) and 50μg anti-Thy1.2 (T24), a dose that efficiently deplete peripheral T cells.

Fetal thymus transplants

Thymic lobes were collected from E15.5 embryos and both lobes from a single embryo were placed under the kidney capsule of the recipient nu/nu mice. Four weeks later, thymic lobes were removed and analyzed.

Statistical analysis

Statistical analysis was performed using students t-test (unpaired, two-tailed). Probability values were classified into four categories: $P>0.05$ (not significant), $0.05\geq P>0.01$ (*), $0.01\geq P>0.001$ (**) and $P\geq 0.0001$ (***).

Results

Thymus cellularity and T lymphopoietic activity are decreased in the absence of Dicer expression in TEC

To study the integrated and global role of miRNA in TEC development and function, we generated mice that lack *dicer1* expression in thymic epithelia. For this purpose, mice with a conditional *dicer1* allele (Dicer$^{fl/fl}$, (14)) were crossed to transgenic animals expressing the Cre recombinase in all TECs (15). Because Cre expression in heterozygote Foxn1-Cre transgenic mice is non-toxic to TECs (Supplemental Fig. 1 and ref (16)), Dicer$^{fl/fl}$ mice negative for the expression of Cre were used as controls and compared to heterozygous Cre-transgenic Dicer$^{fl/fl}$ mice (designated Foxn1-Cre::Dicer$^{fl/fl}$). Thymus cellularity was unaffected in fetal and early post-natal Foxn1-Cre::Dicer$^{fl/fl}$ mice despite a complete deletion of the *dicer1* locus and the absence of distinct miRNA species in TEC at day 16.5 of gestation (E16.5) (Fig. 1A, 1B, 1D). A significant reduction in thymus size and absolute cell number was first observed in three week old Foxn1-Cre::Dicer$^{fl/fl}$ mice (Fig. 1A,1C). In contrast, changes in intrathymic T cell differentiation were already apparent in Foxn1-Cre::Dicer$^{fl/fl}$ mice as early as the first week of life (Fig. 1E, 1F). While the frequency of double negative (DN) cells was increased, CD4^{-}CD8^{+} single positive (SP) thymocytes with a mature phenotype (CD24^{lo}CD3^{hi}) were diminished. At 3 weeks and later, the relative frequency of double positive (DP) thymocytes was consistently increased though all subsequent maturational stages were diminished (Fig. 1E, 1F). By 30 weeks of age, DP thymocytes were almost completely absent in Foxn1-Cre::Dicer$^{fl/fl}$ mice. The competence of Dicer-deficient TEC to support regular T cell development was thus progressively compromised affecting both the generation of DP thymocytes and their subsequent maturation to single positive, naïve T cells.

Commitment to the T cell lineage requires Dicer expression in cTEC

We next investigated the nature of the CD4^{-}CD8^{-} thymocytes as these cells were already increased in Foxn1-Cre::Dicer$^{fl/fl}$ mice as early as 1 week of age and represented more than half of all thethymocytes in 30 week old mutant animals (Fig. 1E). The screening of these cells for the expression of non-T cell lineage markers identified a relative and absolute increase of CD19^{+} cells (Fig. 2A). Although a substantial proportion of these cells expressed high levels of CD93 similar to the pattern observed for B cells in the bone marrow of both wild type and mutant mice (Fig. 2A), they did not express IgM. We therefore conclude that these were immature thymic B cells that developed in situ, possibly due to changes in the microenvironment. Indeed the thymic medulla progressively displayed increased numbers of Lyve-1^{+}lymphatic vessels, PNAd^{+} high endothelial venules and CR-1^{+} follicular dendritic cells (Fig. 2B), that in aggregate resulted in older animals in a histological structure reminiscent of secondary lymphoid tissue.

Since commitment to a T cell fate is dependent on Dll4 expression by cTEC (17), we next tested whether Foxn1-Cre::Dicer$^{fl/fl}$ mice lacked the correct expression of Dll4^{+}. The

relative frequency and absolute cell number of Dll4^{+} cTEC was halvedin 3 week old Foxn1-Cre::Dicer$^{fl/fl}$ mice when compared to controls (Fig. 2C). The relative frequency of early thymic progenitors (ETP, defined as Lin^{-}CD25^{-}CD44^{hi}c-kit^{+} cells) among thymocytes was in parallel decreased by two-fold when compared to age-matched controls (0.02±0.011 vs 0.04±0.017; $p<0.05$, n=4). Thus, Dicer deficient TECs created an altered microenvironment reduced in the molecular cues critical for the attraction of early thymic progenitors and their commitment to the T cell lineage.

Dicer-deficient TEC fail to maintain a regular thymic microenvironment

To further investigate the consequences a TEC-restricted loss of Dicer-dependent miRNA expression, control and mutant thymus tissue sections were analyzed for the composition and organization of their stroma. In 2 day and 3 week old mice of both groups, histological analyses demonstrated well demarcated medullary islands surrounded by a cell-dense cortex (Fig. 3A and Supplemental Fig. 2). In 3 week old mutant mice, the cortical TEC network was however, less dense and, in contrary to the wild type thymus, mainly composed of cytokeratin (CK)5^{+}CK8^{+}, cTEC (MTS10^{-}). The thymic cortex of mutant mice had also changed in as much as its epithelia expressed lower amounts of Psmb11 (a.k.a. β5t), a cTEC-specific component of the thymoproteasome pivotal for the differentiation of MHC class I restricted CD8 SP thymocytes (18) (Fig. 3A, 3B). mTEC (CK5^{+}MTS10^{+}) were reduced in number and mostly located at the cortico-medullary junction. In parallel, ERTR7^{+} fibroblasts had accumulated in the presumed medulla where the few remaining mTEC were usually less reactive with UEA-1 though Aire^{+} epithelia and dendritic cells could still be detected (Fig. 3A and G.N., G.A.H unpublished observation).

The small thymus remnant detected in 30 week old Foxn1-Cre::Dicer$^{fl/fl}$ mice had lost its typical cortico-medullary organization and the few remaining TEC were now arranged in several solitary islands devoid of mTEC contributions (Fig. 3B). Though almost all of the epithelia displayed a cortical phenotype (CK8^{+}MTS10^{-}UEA-1^{-}), the expression of Psmb11 could not anymore be detected. The loss of Dicer expression differentially affected TEC cellularity of Foxn1-Cre::Dicer$^{fl/fl}$ mice, in contrast to absolute mTEC, both absolute and relative cTEC numbers of cTEC were increased (Fig. 3C), a change that correlated with a higher proliferation rate (Fig. 3D). Thus, a lack of Dicer expression in TEC progressively precludes the normal differentiation, patterning, maintenance and function of these cells.

To assess whether miRNAs are specifically required by TEC for MHC expression and their differentiation from immature (MCH^{lo}) to mature (MHC^{hi}) mTEC, we next analyzed TEC for their MHCII expression and mTEC for the detection of the autoimmune regulator (Aire). Both cTEC and mTEC from Foxn1-Cre::Dicer$^{fl/fl}$ and Dicer$^{fl/fl}$ mice expressed comparable amounts of MHC class I and II molecules (Fig. 3E). However, the relative frequency of MHCII^{lo}Aire^{-} mTEC was reduced and that of MHCII^{hi}Aire^{-} and MHCII^{hi}Aire^{+} mTEC was increased in Foxn1-Cre::Dicer$^{fl/fl}$ mice. Thus, miRNAs appear to be required for the regular maintenance of MHCII^{lo} mTEC but dispensable for their differentiation into MHCII^{hi}Aire^{+} mTEC, which express an array of peripheral tissue-specific antigens (PTA) and are critical for negative selection of maturing thymocytes (see below).

Dicer-deficient cTEC fail to impose efficient positive selection

Given the changes in cTEC we next investigated in Foxn1-Cre::Dicer$^{fl/fl}$ and control mice the sequential changes in thymocyte CD3 and CD69 cell surface expressions as phenotypic markers of positive selection (19). Under physiological conditions, positive selection sets off a transient up-regulation of CD69 among CD3^{int} DP thymocytes. In turn, these cells sequentially adopt a CD3^{hi}CD69^{+} and eventually a CD3^{hi}CD69^{-} cell surface phenotype. The relative frequencies of these distinct thymocyte populations were undisturbed in 1 week

old Foxn1-Cre::Dicer$^{fl/fl}$ mice implying thymocyte positive selection to be normal (Fig. 4A). In contrast, 2 week and older mutant mice displayed a progressively compromised positive selection as the frequencies of their CD3^{int}CD69^{+} and CD3^{hi}CD69^{+} DP thymocytes were gradually reduced (Fig. 4A) despite an increased frequency of cTEC (Fig. 3C). To detail early post-selection steps in DP thymocyte differentiation, we also analyzed changes in CD4 and CD8 expression on either CD3^{int}CD69^{+} or CD3^{hi}CD69^{+}DP cells (Fig. 4B). Although the downregulation of CD8 on CD3^{int}CD69^{+} cells occurred normally in 1 and 2 week old Foxn1-Cre::Dicer$^{fl/fl}$ mice, this was impaired in 3 week old mutants (Fig. 4B, left panels). Focusing on younger Foxn1-Cre::Dicer$^{fl/fl}$ mice with a seemingly undisturbed cortical epithelial microenvironment, we also noticed a gradual defect in the progression of CD3^{hi}CD69^{+} DP thymocytes (via the intermediate CD8^{hi}CD4^{lo} stage) to cells with a mature SP CD8 phenotype (Fig. 4B, right panels). Thus, positive selection of DP thymocytes is significantly impaired in Foxn1-Cre::Dicer$^{fl/fl}$ mice as early as the second week of life and is preceded by a defect in DP maturational progression towards the CD8 SP lineage.

Since Dicer-deficient mice express an impaired thymoproteasome (Fig. 3A), we next investigated the development of MHC class I restricted thymocytes expressing a T cell antigen receptor known to depend on Psmb11 expression for its efficient positive selection (20). For this purpose, sub-lethally irradiated neonatal Foxn1-Cre::Dicer$^{fl/fl}$and Dicer$^{fl/fl}$mice were engrafted with day 14 fetal liver cells from OT-I TCR transgenic mice. The OT-I TCR (composed of the Vα2 and Vβ5 chains) recognizes ovalbumin and is selected by self-peptides derived from β-catenin and other proteins (21). The selection of OT-I TCR transgenic thymocytes was severely compromised in chimeric Foxn1-Cre::Dicer$^{fl/fl}$mice and this resulted in a significant reduction of cells with an immediate post-selection phenotype, i.e. CD4^{hi}CD8^{int} and CD4^{neg}CD8^{hi} (Fig. 4C). The partial block in positive selection resulted in parallel in an increase in pre-selection DP thymocytes and a concomitant reduction in OT-I transgenic T cells committed to the CD8 lineage(Fig. 4C, left and middle panel). Moreover, chimeric Foxn1-Cre::Dicer$^{fl/fl}$ mice displayed a reduced frequency of mature transgenic SP CD8 thymocytes expressing high surface Vα2 concentrations (Fig. 4C, right panel). Taken together, the absence of Dicer expression in TEC resulted in reduced positive thymocyte selection and an altered antigen receptor repertoire.

To test whether the thymus phenotype in Foxn1-Cre::Dicer$^{fl/fl}$ mice was affected by Foxn1-Cre mediated recombination in keratinocytes and consequent systemic influences, we transplanted embryonic thymic tissue from both Dicer$^{fl/fl}$ and Foxn1-Cre::Dicer$^{fl/fl}$ mice under the kidney capsule of a nu/nu recipients. Analysis of the grafted tissue 4 weeks after transplantation revealed a phenotype identical to that observed in age-matched Foxn1-Cre::Dicer$^{fl/fl}$ mice (Supplemental Fig. 3A–C). This finding is in keeping with the observation that Foxn1-Cre::Dicer$^{fl/fl}$ mice have a normal skin (Supplemental Fig. 3D).

Gene expression analysis in Dicer-deficient TEC uncover miRNA-sensitive cellular processes

Gene expression profiles were established for both cortical and medullary TEC subpopulations to identify transcripts that are significantly up- or down-regulated as a consequence of Dicer deficiency (Fig. 5A, 5B). For this purpose, Foxn1-Cre::Dicer$^{fl/fl}$ and Dicer$^{fl/fl}$mice were investigated at two weeks of age since the former animals still had a relatively intact cTEC cellularity though already displayed functional deficiencies. Gene Ontology (GO) analysis of significantly upregulated and downregulated transcripts (corrected $p<0.05$) predicted multiple cellular processes to be affected in cortical, medullary and both types of TEC (Fig. 5C, 5D). Specifically, transcription, cell signaling, differentiation, adhesion, apoptosis and the organization of extracellular matrix were predicted to be altered as a consequence of Dicer deficiency in TEC.

Dicer-deficiency in TEC alters peripheral T cell phenotype

The lack of Dicer expression in TEC led to significant phenotypic changes among peripheral T cells. Both naïve $CD4^+$ and $CD8^+$ T cells (i.e. $CD62L^{hi}CD44^-$) were reduced in Foxn1-Cre::$Dicer^{fl/fl}$ mice at 8 weeks of age whilst the relative frequency of memory T cells was two- to three-fold more abundant, a finding likely caused by moderate T lymphopenia (Fig. 6A, 6B). Moreover, Foxn1-Cre::$Dicer^{fl/fl}$ mice displayed a proportional increase in $CD8^+$effector ($CD44^{hi}CD62L^{low/-}$)and central memory ($CD44^{hi}CD62L^{hi}$)T cells. In keeping with the degree of lymphopenia, the relative frequency of $FoxP3^+CD4^+$ regulatory T cells was only modestly increased though their cellularity was not significantly different from that of $Dicer^{fl/fl}$ mice (Fig. 6C).

T cells selected in a thymus with Dicer deficient TEC elicit autoimmunity

We next examined whether T cells selected by Foxn1-Cre::$Dicer^{fl/fl}$mice were prone to elicit autoimmunity since their selection was altered by thymic microenvironmental changes possibly resulting in a T cell repertoire with different functional properties. Although Foxn1-Cre::$Dicer^{fl/fl}$ mice were followed and regularly analyzed for as long as 45 weeks, spontaneous lymphocytic organ infiltrates were not observed at a frequency different to that of control mice (unpublished observations). As peripheral tolerance may have been maintained in Foxn1-Cre::$Dicer^{fl/fl}$mice by T cells that had early on developed in a yet largely normal though already miRNA-deficient thymic epithelial microenvironment (22), mutant and wild type mice were efficiently T cell depleted at the age of 2 weeks using a mixture of anti-CD4, -CD8 and -Thy1.2 antibodies. In the course of autologous reconstitution, newly formed T cells were now selected in a thymic microenvironment which in the case of Foxn1-Cre::$Dicer^{fl/fl}$ mice had adopted an altered architecture and had lost its capacity for normal TCR selection. Multi-organ infiltration developed in Foxn1-Cre::$Dicer^{fl/fl}$ but not control mice over the course of 28 weeks, variably affecting eyes, pancreas, salivary glands, and liver (Fig. 7A). The inflammatory cell infiltrations of the eyes altered the retinal architecture in its entire thickness leading to a partial destruction of the photoreceptor outer segment and the nuclear layer.

As thymic expression of self-antigens is critical for the maintenance of self tolerance, transcripts for selective single self-antigens were quantified in purified mTEC of 2 week old Foxn1-Cre::$Dicer^{fl/fl}$and $Dicer^{fl/fl}$ mice (Fig. 7B, 7C). This time point had specifically been chosen since the relative frequency of $MHCII^{hi}Aire^+$ mTEC was comparable for both mouse strains (Fig. 3F). A significant decrease in both Aire-dependent and -independent transcripts was detected with retinal (IRbp), salivary gland (Salivary protein 1, Spt1), hepatic (C-reactive protein, CRP) and pancreatic (Insulin-2, Ins2; Glutamic acid decarboxylase, Gad1) peripheral tissue antigens (PTA) invariably reduced in Dicer-deficient mTEC (Fig. 7B, 7C and 7D). These changes correlated with the pattern of tissue infiltrations linking defects in PTA expression to organ-specific autoimmune pathologies.

Discussion

Short, non-coding RNAs typically modulate the regulation of organ development via subtle though efficient parallel targeting of multiple components within a regulatory network (10,23). Because the molecular targets of most miRNA remain experimentally unverified, their role in tissue differentiation and function has largely been interrogated via global interference with their biogenesis (5). Here, the dependence of TEC differentiation and function on the biological properties of miRNA has been investigated in mice where Dicer is ablated after formation of the thymus primordium but before the complete patterning of its microenvironment. Our results reveal that miRNA are differentially expressed in separate

TEC subpopulations and that this non-coding species of RNA is essential for the maintenance of a regularly composed and correctly functioning thymic microenvironment.

The TEC-targeted, embryonic loss of Dicer results in a sequential emergence of structural and functional alterations with defects apparent only after the first week of life. The asynchronous appearance of a complex phenotype is likely the result of a substantial variation in the decay of individual miRNA following *dicer1* gene ablation (24) and may also reflect a variable susceptibility of separate TEC subpopulations for the loss of specific miRNA.

The hematopoietic cells settling into the thymus require signals from Dll4 expressed by cTEC for their commitment to a T cell fate (17). In the absence of Dicer, fewer cTEC express Dll4 which suggestDll4 as a likely indirect target of miRNA. Diminished expression of Dll4 on cTEC correlates with the observed reduction of ETPs and a robust B cell differentiation *in situ.* Since the Notch ligand density is important *in vitro* for the commitment of hematopoietic precursors to a T cell fate (25), quantitative signaling differences suffice to explain the *in situ* B cell development in younger Foxn1-Cre::Dicer$^{fl/fl}$ mice. These findings provide a molecular mechanism (i.e. reduced Dll4 expression by cTEC)for the increase in intrathymic B-cell development (this report and ref. (26))

In older mutant animals, the microenvironment is unable to attract uncommitted hematopoietic precursors and consequently neither immature B nor T cells can be detected. Rather, the cellular composition and organization of the microenvironment demonstrates a structure reminiscent of secondary lymphoid tissues where lymphocyte homing is directed through PNAd^{+} venules (27) and new lymphatic vessels are established (in the absence of overt inflammation) possibly sprouting from pre-existing endothelial cells (28). The increase and persistence of the two vascular systems is likely mediated by different mechanisms including the presence of B cells, the expression of CCL21 by TEC and dendritic cells, and the stimulation of the lymphotoxin beta receptor on endothelial cells of blood and lymph vessels (29,30).

The almost complete attrition of TEC is an intriguing feature of older Foxn1-Cre::Dicer$^{fl/fl}$ mice. Given that miRNA expression patterns create a cell type-specific signature and help to reinforce cell fate specifications, it is conceivable that the pool of TEC precursor/stem cells is altered and/or that their differentiation into distinct TEC subsets is repressed following the targeted loss of Dicer expression. A reduction of MHC^{lo} mTEC suggests a defective maintenance of the progenitor pool in the absence of miRNA, a finding that is contrasting the higher frequency of p63^{+} TEC reported recently (26). The changes in gene expression in miRNA-deficient TECs infer that several pathways essential for cell pluripotency, differentiation and survival appear to be affected following the loss of Dicer. Indeed, the continuous replacement of immature and mature TEC was severely affected in older Foxn1-Cre::Dicer$^{fl/fl}$ mice. The loss of miRNA also resulted in the upregulation of multiple transcripts of key molecules known to affect TEC development and function. For example the correct control of Wnt signaling in TECs is required for thymus development since gain of canonical Wnt signaling activity is incompatible with regular thymus organogenesis and function (15). Similarly, changes in BMP signaling in TEC affect both embryonic development (31) and thymopoietic function (32). Increased TgfβR3 expression in Dicer deficient TECs possibly contributes to the enhanced thymic involution via enhanced stimulation of TgfβR2 signaling (16), whereas the upregulation of insulin-like growth factor 1 receptor (Igf-1R) may, in response to Igf-1, account for increased TEC proliferation (Fig. 3D; and ref. (33)). Hence, distinct miRNA may directly control the expression, activation and/or availability of signaling elements essential for either TEC differentiation, proliferation or function. In keeping with this contention, the single loss of miR-29a

enhances thymic involution in adult mice though neither thymic architecture nor function are affected (26).

Thymocyte differentiation such as the generation of post-selection thymocytes with a $CD3^{hi}CD69^{+}CD4^{-}CD8^{+}$is already impaired in young Foxn1-Cre::$Dicer^{fl/fl}$ mice even though cellularity, MHC expression and architectural organization of the cTEC scaffold has not yet been compromised. This finding infers a previously unnoticed (26)qualitative cTEC deficiency in supporting the development of CD8 SP thymocytes. Later in life, mutant mice display a defect in positive selection that is marked by a partial block in the sequential upregulation of CD69 and CD3 on DP thymocytes. This fault points to a previously unrecognized critical element in positive selection since neither MHC nor Psmb11 are affected when the deficiency becomes first apparent (18,34–37). Though a reduced density of the epithelial network is likely to contribute to altered thymocyte development in older mice (26), overt TEC-free areas as observed in Kremen1-deficient mice were not sufficient to compromise T cell development (38). The continued selection of $CD3^{hi}CD69^{+}$ thymocytes and their differentiation along the SP CD8 lineage is MHC independent but requires other, additional cues (39–41). However, only few candidate molecules expressed by cTEC including ICAM and IL-7 (42,43)have so far been inferred to play a role in positive thymocyte selection, yet their transcripts remained unchanged in Dicer-deficient cTEC (unpublished observations). Thus, mice that lack Dicer expression in cTEC display significant defects in thymocyte development which appear to be unrelated to previously identified mechanisms controlling this multi-stage process.

Thymocyte negative selection is likely impaired in Foxn1-Cre::$Dicer^{fl/fl}$ mice since their mTEC display a significant deficiency in promiscuous gene expression. The molecular signature of this defect implies a common yet undefined mechanism that controls some but not all known PTA transcripts. Though the differentiation of $Aire^{+}$ mTEChi was apparently independent of miRNAs, the expression of a significant number of Aire dependent PTAs was, however, affected by the lack of Dicer expression. It is thus conceivable that miRNAs may act either in concert or downstream of Aire to regulate the expression of a subset of Aire-dependent PTAs. In parallel, our data likewise reveal that miRNA also control the expression of a number of Aire-independent PTA, possibly via a common pathway. As a corollary, central tolerance induction is defective and autoimmunity ensues. Because PTA expression confined to the perinatal period suffices to induce long-lasting tolerance (22), functionally relevant defects in negative selection become only apparent once the initially chosen T cell pool is replaced by cells selected in the distorted thymic microenvironment of two and more week old Foxn1-Cre::$Dicer^{fl/fl}$ mice. The pattern of organ-specific autoimmunity observed in these mice correlates with the altered expression profile of tissue-specific self-antigens. It is therefore conceivable that some forms of autoimmunity may also occur as a consequence of known or not yet described miRNA polymorphisms that either affect the biogenesis of miRNA or influence their ability for target repression.

Supplementary Material

Refer to Web version on PubMed Central for supplementary material.

Acknowledgments

Financial support: This work was supported by the Swiss National Science Foundation Grants 3100-68310.02 and 3100-122558 (to G.A.H.). APM and RNC were partially funded by the Spanish Minister of Science and Innovation (BIO2010-17527) and Madrid government grant (P2010/BMD-2305); RNC acknowledges Juan de la Cierva program for economical support.

The authors thank Katrin Hafen, Annick Peter, Philippe Demougin, Rodrigo Recinos, and Angelika Offinger for excellent technical support, Mary Deadman for critically reading the manuscript, and Sabrina Harris for secretarial assistance.

Abbreviations used in this article

TEC	thymic epithelial cell
mTEC	medullary TEC
cTEC	cortical TEC
DN	double negative
DP	double positive
SP	single positive
E	embryonic day
miRNA	micro RNA
PTA	peripheral tissue antigen

References

1. Klein L, Hinterberger M, Wirnsberger G, Kyewski B. Antigen presentation in the thymus for positive selection and central tolerance induction. Nat Rev Immunol. 2009; 9:833–844. [PubMed: 19935803]
2. Klug DB, Carter C, Crouch E, Roop D, Conti CJ, Richie ER. Interdependence of cortical thymic epithelial cell differentiation and T-lineage commitment. Proc Natl Acad Sci U S A. 1998; 95:11822–11827. [PubMed: 9751749]
3. Gray DH, Seach N, Ueno T, Milton MK, Liston A, Lew AM, Goodnow CC, Boyd RL. Developmental kinetics, turnover and stimulatory capacity of thymic epithelial cells. Blood. 2006; 108:3777–3785. [PubMed: 16896157]
4. Takahama Y. Journey through the thymus: stromal guides for T-cell development and selection. Nat Rev Immunol. 2006; 6:127–135. [PubMed: 16491137]
5. Bartel DP. MicroRNAs: target recognition and regulatory functions. Cell. 2009; 136:215–233. [PubMed: 19167326]
6. Kim VN. MicroRNA biogenesis: coordinated cropping and dicing. Nat Rev Mol Cell Biol. 2005; 6:376–385. [PubMed: 15852042]
7. Lewis BP, Burge CB, Bartel DP. Conserved seed pairing, often flanked by adenosines, indicates that thousands of human genes are microRNA targets. Cell. 2005; 120:15–20. [PubMed: 15652477]
8. Baek D, Villén J, Shin C, Camargo FD, Gygi SP, Bartel DP. The impact of microRNAs on protein output. Nature. 2008; 455:64–71. [PubMed: 18668037]
9. Selbach M, Schwanhäusser B, Thierfelder N, Fang Z, Khanin R, Rajewsky N. Widespread changes in protein synthesis induced by microRNAs. Nature. 2008; 455:58–63. [PubMed: 18668040]
10. Xiao C, Rajewsky K. MicroRNA control in the immune system: basic principles. Cell. 2009; 136:26–36. [PubMed: 19135886]
11. Benjamini Y, Hochberg Y. Controlling the false discovery rate: a practical and powerful approach to multiple testing. Journal of the Royal Statistical Society. 1995; 57:289–300.
12. Nogales-Cadenas R, Carmona-Saez P, Vazquez M, Vicente C, Yang X, Tirado F, Carazo JM, Pascual-Montano A. GeneCodis: interpreting gene lists through enrichment analysis and integration of diverse biological information. Nucleic Acids Res. 2009; 37:W317–W322. [PubMed: 19465387]
13. Carmona-Saez P, Chagoyen M, Tirado F, Carazo JM, Pascual-Montano A. GENECODIS: a web-based tool for finding significant concurrent annotations in gene lists. Genome Biol. 2007; 8:R3. [PubMed: 17204154]

14. Harfe BD, McManus MT, Mansfield JH, Hornstein E, Tabin CJ. The RNaseIII enzyme Dicer is required for morphogenesis but not patterning of the vertebrate limb. Proc Natl Acad Sci U S A. 2005; 102:10898–10903. [PubMed: 16040801]
15. Zuklys S, Gill J, Keller MP, Hauri-Hohl M, Zhanybekova S, Balciunaite G, Na KJ, Jeker LT, Hafen K, Tsukamoto N, Amagai T, Taketo MM, Krenger W, Holländer GA. Stabilized {beta}-Catenin in Thymic Epithelial Cells Blocks Thymus Development and Function. J Immunol. 2009; 182:2997–3007. [PubMed: 19234195]
16. Hauri-Hohl MM, Zuklys S, Keller MP, Jeker LT, Barthlott T, Moon AM, Roes J, Holländer GA. TGF-beta signaling in thymic epithelial cells regulates thymic involution and postirradiation reconstitution. Blood. 2008; 112:626–634. [PubMed: 18474727]
17. Hozumi K, Mailhos C, Negishi N, Hirano KI, Yahata T, Ando K, Zuklys S, Holländer GA, Shima DT, Habu S. Delta-like 4 is indispensable in thymic environment specific for T cell development. J Exp Med. 2008; 205:2507–2513. [PubMed: 18824583]
18. Murata S, Sasaki K, Kishimoto T, Niwa S, Hayashi H, Takahama Y, Tanaka K. Regulation of CD8+ T cell development by thymus-specific proteasomes. Science. 2007; 316:1349–1353. [PubMed: 17540904]
19. Barthlott T, Kohler H, Eichmann K. Asynchronous coreceptor downregulation after positive thymic selection: prolonged maintenance of the double positive state in CD8 lineage differentiation due to sustained biosynthesis of the CD4 coreceptor. J Exp Med. 1997; 185:357–362. [PubMed: 9016884]
20. Nitta T, Ohigashi I, Nakagawa Y, Takahama Y. Cytokine crosstalk for thymic medulla formation. Curr Opin Immunol. 2010; 23:190–197. [PubMed: 21194915]
21. Santori FR, Brown SM, Vukmanović S. Genomics-based identification of self-ligands with T cell receptor-specific biological activity. Immunol Rev. 2002; 190:146–160. [PubMed: 12493012]
22. Guerau-de-Arellano M, Martinic M, Benoist C, Mathis D. Neonatal tolerance revisited: a perinatal window for Aire control of autoimmunity. J Exp Med. 2009; 206:1245–1252. [PubMed: 19487417]
23. Tsitsiou E, Lindsay MA. microRNAs and the immune response. Curr Opin Pharmacol. 2009; 9:514–520. [PubMed: 19525145]
24. Soukup GA, Fritzsch B, Pierce ML, Weston MD, Jahan I, McManus MT, Harfe BD. Residual microRNA expression dictates the extent of inner ear development in conditional Dicer knockout mice. Dev Biol. 2009; 328:328–341. [PubMed: 19389351]
25. Dallas MH, Varnum-Finney B, Delaney C, Kato K, Bernstein ID. Density of the Notch ligand Delta1 determines generation of B and T cell precursors from hematopoietic stem cells. J Exp Med. 2005; 201:1361–1366. [PubMed: 15851488]
26. Papadopoulou AS, Dooley J, Linterman MA, Pierson W, Ucar O, Kyewski B, Zuklys S, Hollander GA, Matthys P, Gray DH, De Strooper B, Liston A. The thymic epithelial microRNA network elevates the threshold for infection-associated thymic involution via miR-29a mediated suppression of the IFN-α receptor. Nat Immunol. 2012; 13:181–187. [PubMed: 22179202]
27. Girard JP, Springer TA. High endothelial venules (HEVs): specialized endothelium for lymphocyte migration. Immunol Today. 1995; 16:449–457. [PubMed: 7546210]
28. He Y, Rajantie I, Ilmonen M, Makinen T, Karkkainen MJ, Haiko P, Salven P, Alitalo K. Preexisting lymphatic endothelium but not endothelial progenitor cells are essential for tumor lymphangiogenesis and lymphatic metastasis. Cancer Res. 2004; 64:3737–3740. [PubMed: 15172976]
29. Liao S, Ruddle NH. Synchrony of high endothelial venules and lymphatic vessels revealed by immunization. J Immunol. 2006; 177:3369–3379. [PubMed: 16920978]
30. Muniz LR, Pacer ME, Lira SA, Furtado GC. A Critical Role for Dendritic Cells in the Formation of Lymphatic Vessels within Tertiary Lymphoid Structures. J Immunol. 2011; 187:828–834. [PubMed: 21666055]
31. Bleul CC, Boehm T. BMP Signaling Is Required for Normal Thymus Development. J Immunol. 2005; 175:5213–5221. [PubMed: 16210626]
32. Tsai PT, Lee RA, Wu H. BMP4 acts upstream of FGF in modulating thymic stroma and regulating thymopoiesis. Blood. 2003; 102:3947–3953. [PubMed: 12920023]

33. Chu YW, Schmitz S, Choudhury B, Telford W, Kapoor V, Garfield S, Howe D, Gress RE. Exogenous insulin-like growth factor 1 enhances thymopoiesis predominantly through thymic epithelial cell expansion. Blood. 2008; 112:2836–2846. [PubMed: 18658030]
34. Grusby MJ, Johnson RS, Papaioannou VE, Glimcher LH. Depletion of $CD4^+$ T cells in major histocompatibility coplex class II-deficient mice. Science. 1991; 253:1417–1420. [PubMed: 1910207]
35. Cosgrove D, Gray D, Dierich A, Kaufman J, Lemeur M, Benoist C, Mathis D. Mice lacking MHC class II molecules. Cell. 1991; 66:1051–1066. [PubMed: 1909605]
36. Zijlstra M, Bix M, Simister NE, Loring JM, Raulet DH, Jaenisch R. β2-Microglobulin deficient mice lack CD4–8^+ cytolytic T cells. Nature. 1990; 344:742–746. [PubMed: 2139497]
37. Koller BH, Marrack P, Kappler JW, Smithies O. Normal development of mice deficient in β2M, MHC class I proteins and $CD8^+$ T cells. Science. 1990; 248:1227–1231. [PubMed: 2112266]
38. Osada M, Ito E, Fermin HA, Vazquez-Cintron E, Venkatesh T, Friedel RH, Pezzano M. The Wnt signaling antagonist Kremen1 is required for development of thymic architecture. Clin Dev Immunol. 2006; 13:299–319. [PubMed: 17162372]
39. Muller KP, Kyewski BA. T cell receptor targeting to thymic cortical epithelial cells in vivo induces survival, activation and differentiation of immature thymocytes. European Journal of Immunology. 1993; 1993:1661–1670. [PubMed: 8100778]
40. Hare KJ, Jenkinson EJ, Anderson G. CD69 expression discriminates MHC-dependent and -independent stages of thymocyte positive selection. J Immunol. 1999; 162:3978–3983. [PubMed: 10201918]
41. Singer A, Adoro S, Park JH. Lineage fate and intense debate: myths, models and mechanisms of CD4- versus CD8-lineage choice. Nat Rev Immunol. 2008; 8:788–801. [PubMed: 18802443]
42. Paessens LC, Singh SK, Fernandes RJ, van Kooyk Y. Vascular cell adhesion molecule-1 (VCAM-1) and intercellular adhesion molecule-1 (ICAM-1) provide co-stimulation in positive selection along with survival of selected thymocytes. Molecular immunology. 2008; 45:42–48. [PubMed: 17604837]
43. Park JH, Adoro S, Guinter T, Erman B, Alag AS, Catalfamo M, Kimura MY, Cui Y, Lucas PJ, Gress RE, Kubo M, Hennighausen L, Feigenbaum L, Singer A. Signaling by intrathymic cytokines, not T cell antigen receptors, specifies CD8 lineage choice and promotes the differentiation of cytotoxic-lineage T cells. Nat Immunol. 2010; 11:257–264. [PubMed: 20118929]

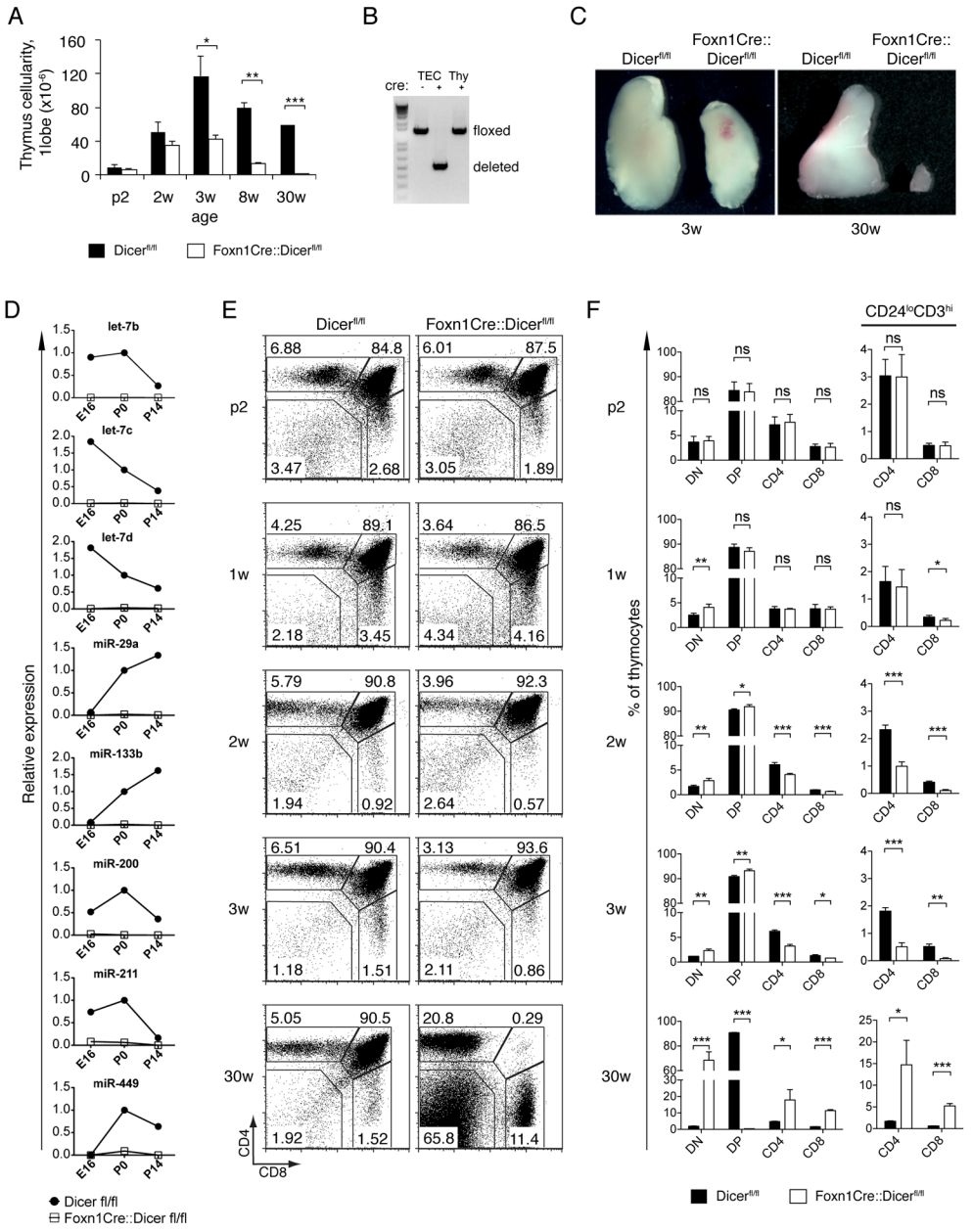

FIGURE 1.

Reduced thymic cellularity and gradual failure of T cell development in Foxn1-Cre::Dicer$^{fl/fl}$ mice. (A) Total thymic cell numbers of Dicer$^{fl/fl}$ (black bars) and Foxn1-Cre::Dicer$^{fl/fl}$ (white bars) mice at indicated ages (p: post-natal days; w: weeks); *denotes p<0.05; ** p<0.01; *** p<0.001. (B) PCR-based detection of the conditional *dicer1*locus in purified thymocytes (Thy) and TECs from Dicer$^{fl/fl}$ (*cre* −) and Foxn1-Cre::Dicer$^{fl/fl}$ (*cre*+) embryos at day 16.5 (E16.5). (C) Macroscopic analysis of single thymus lobes from 3 and 30 week old Dicer$^{fl/fl}$ and Foxn1-Cre::Dicer$^{fl/fl}$ mice. (D) Decreased miRNA expression in TECs from Foxn1-Cre::Dicer$^{fl/fl}$mice. TECs (CD45-EpCAM+) were isolated by cell sorting from Dicer$^{fl/fl}$(closed circles) and Foxn1-Cre::Dicer$^{fl/fl}$(open squares) mice at the indicated ages and were subjected to quantitative RT-PCR analysis using primers specific for the indicated mature miRNAs. Small nuclear RNA U6 was used as an endogenous control. Data

were normalized to the expression of miRNA in newborn (P0) Dicer$^{fl/fl}$ mice. (E) Flow cytometric analysis for the cell surface expression of CD4 and CD8 on thymocytes isolated from Dicer$^{fl/fl}$ and Foxn1-Cre::Dicer$^{fl/fl}$ mice at indicated ages. Numbers denote the percentage of cells within the given gates in a representative experiment. (F) Frequencies of thymocyte subpopulations (left panel) and of mature (i.e. CD3^{hi}CD24^{lo}) CD4 and CD8 single positive thymocytes (right panel) in Dicer$^{fl/fl}$ (black bars) and Foxn1-Cre::Dicer$^{fl/fl}$ mice (white bars) at indicated ages. Data signify the mean ± SD; ns, not significant; *denotes $p<0.05$; ** $p<0.01$; *** $p<0.001$. Data are representative of at least two independent experiments for each time point with at least three mice per group.

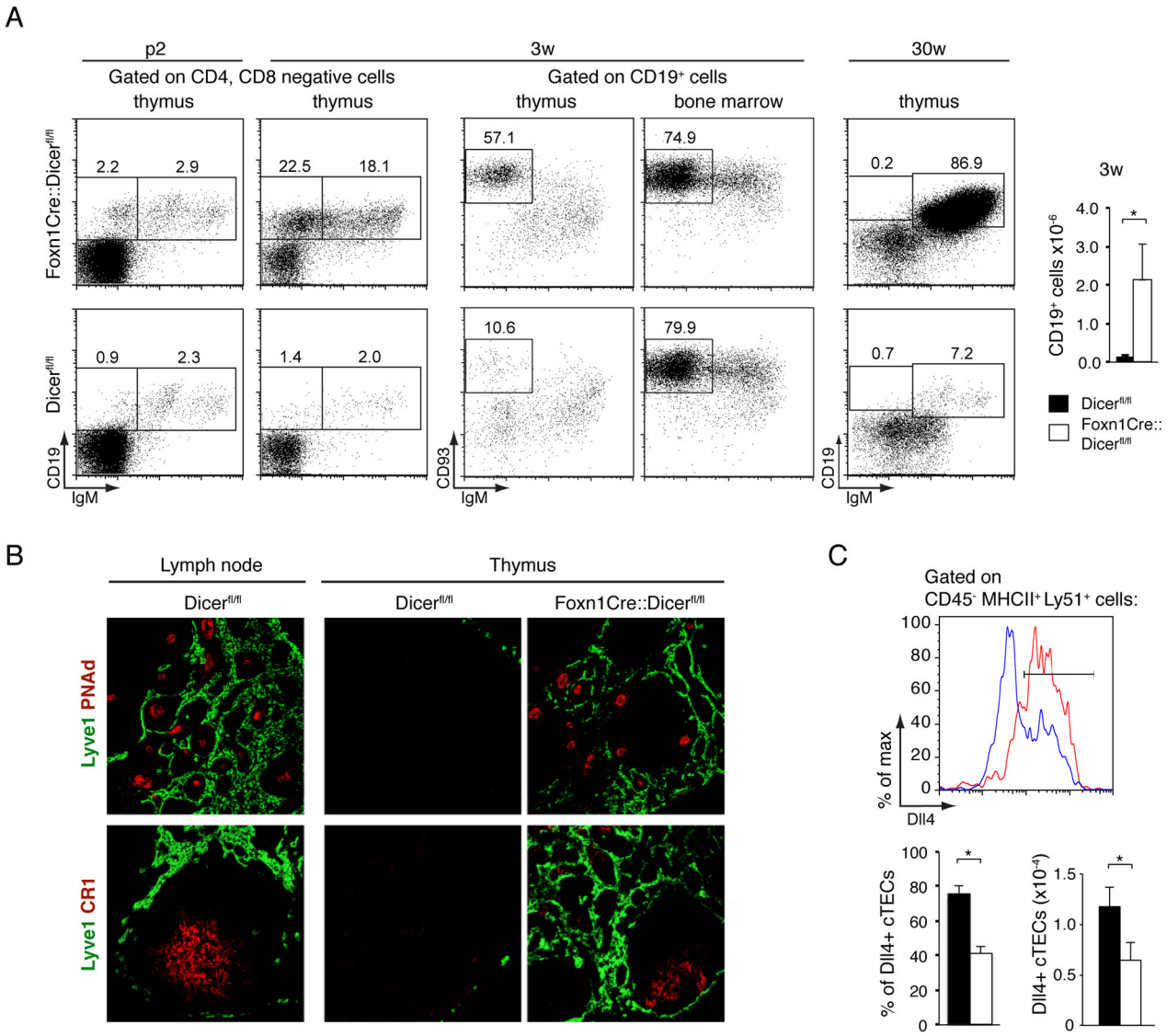

FIGURE 2.

Dicer-deficient TEC create a microenvironment permissive for *in-situ* B-cell development. (A) Left panels: Flow cytometry of $CD4^{-}CD8^{-}$ double negative cells from thymus and bone marrow for the expression of CD19, IgM, and CD93. Numbers denote the frequency observed in a representative experiment for each of the indicated subpopulations. Right panel: Absolute numbers of thymic $CD19^{+}$ cells in 3 week old $Dicer^{fl/fl}$ (black bars) and Foxn1-Cre::$Dicer^{fl/fl}$ (white bars) mice. * denotes $p<0.05$. Three independent experiments with at least 3 mice per group were performed. (B) Immunofluorescence analysis of lymph node and thymus tissue from 30week old mice for the expression of lymphatic vessel endothelial hyaluronan receptor Lyve-1 (identifying lymphatics), peripheral lymph node address in PNAd (staining high endothelial venules) and complement receptor CR1(detecting follicular dendritic cells). Data are representative of at least two separate experiments using each two mice each.(C) FACS analysis of Delta-like 4 (Dll4) expression by cTEC($CD45^{-}MHCII^{+}UEA\text{-}1^{-}Ly51^{+}$) in 3 week old $Dicer^{fl/fl}$ (red line) and Foxn1-Cre::$Dicer^{fl/fl}$ (blue line) mice (upper panel); relative frequency and cellularity of $Dll4^{+}$

cTEC(lower panels); Data signify the mean ± SD; *denotes $p<0.05$. Two independent experiments with at least 3 mice per group were performed.

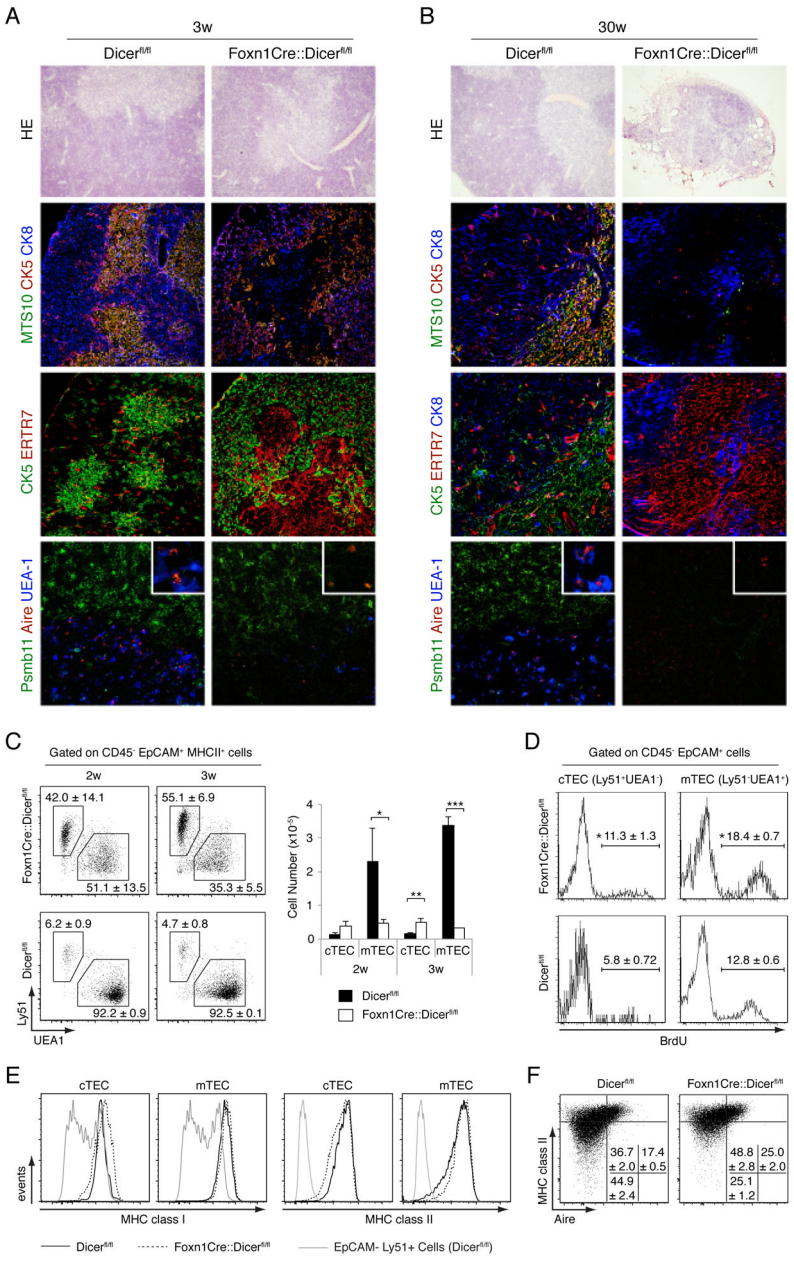

FIGURE 3.

Dicer deficient TEC fail to maintain a regular thymic microenvironment. Hematoxilin and eosin (HE) staining (top row) and immunofluorescence analysis of thymic tissue sections from 3 week old (A) and 30 week old (B) Dicer$^{fl/fl}$ or Foxn1-Cre::Dicer$^{fl/fl}$ mice. For immunohistology, antibodies specific for ERTR7 were used to identify fibroblasts, CK8 and Psmb11 for the detection of cTEC, and MTS10, CK5, and Aire as well as reactivity with UEA-1 for the identification of mTEC. Original magnification 20x; the bottom panels display close-ups in the right upper corner. Data are representative of at least three separate experiments with at least two mice each. (C) Flow cytometric analysis of TEC (CD45^{-}EpCAM^{+}MHCII^{+}) subpopulations isolated from 2 and 3 week old mice. The relative frequency (left panels) and absolute cell numbers (right graph) of cTEC (UEA^{-}1-Ly51^{+}) and mTEC (UEA-1^{+}Ly51^{-}) in Dicer$^{fl/fl}$ (black bars)and Foxn1-Cre::Dicer$^{fl/fl}$ (white bars)

mice are shown. Data indicate the mean ± SD of at least 3 mice per group; *denotes $p<0.05$; ** $p<0.01$; *** $p<0.001$. Data are representative of three independent experiments.(D) BrdU incorporation in cTEC and mTEC isolated from 2 week old $Dicer^{fl/fl}$ and Foxn1-Cre::$Dicer^{fl/fl}$ mice pulsed for 4 hours. The percentage of TEC incorporating the label (mean ± SD, *denotes $p<0.05$; 3 mice per group) is shown. Data are representative of at least two separate experiments. (E) MHC cell surface expression on Dicer deficient TEC. Cortical and medullary thymic epithelial cells from $Dicer^{fl/fl}$ (solid lines) and Foxn1-Cre::$Dicer^{fl/fl}$ (dotted lines) mice were stained for the cell surface expression of MHC class I (left panels) and MHC class II molecules (right panels) and analyzed by flow cytometry. The histograms are representative of two independent experiments with three mice per group.(F) Flow cytometric analysis of MHCII and autoimmune regulator (Aire) expression in TECs ($CD45^{-}EpCAM^{+}$) isolated from 2 week old mice. Numbers denote the percentage of cells (mean ±SD) within the given quadrant. The plots are representative of two independent experiments with three mice per group.

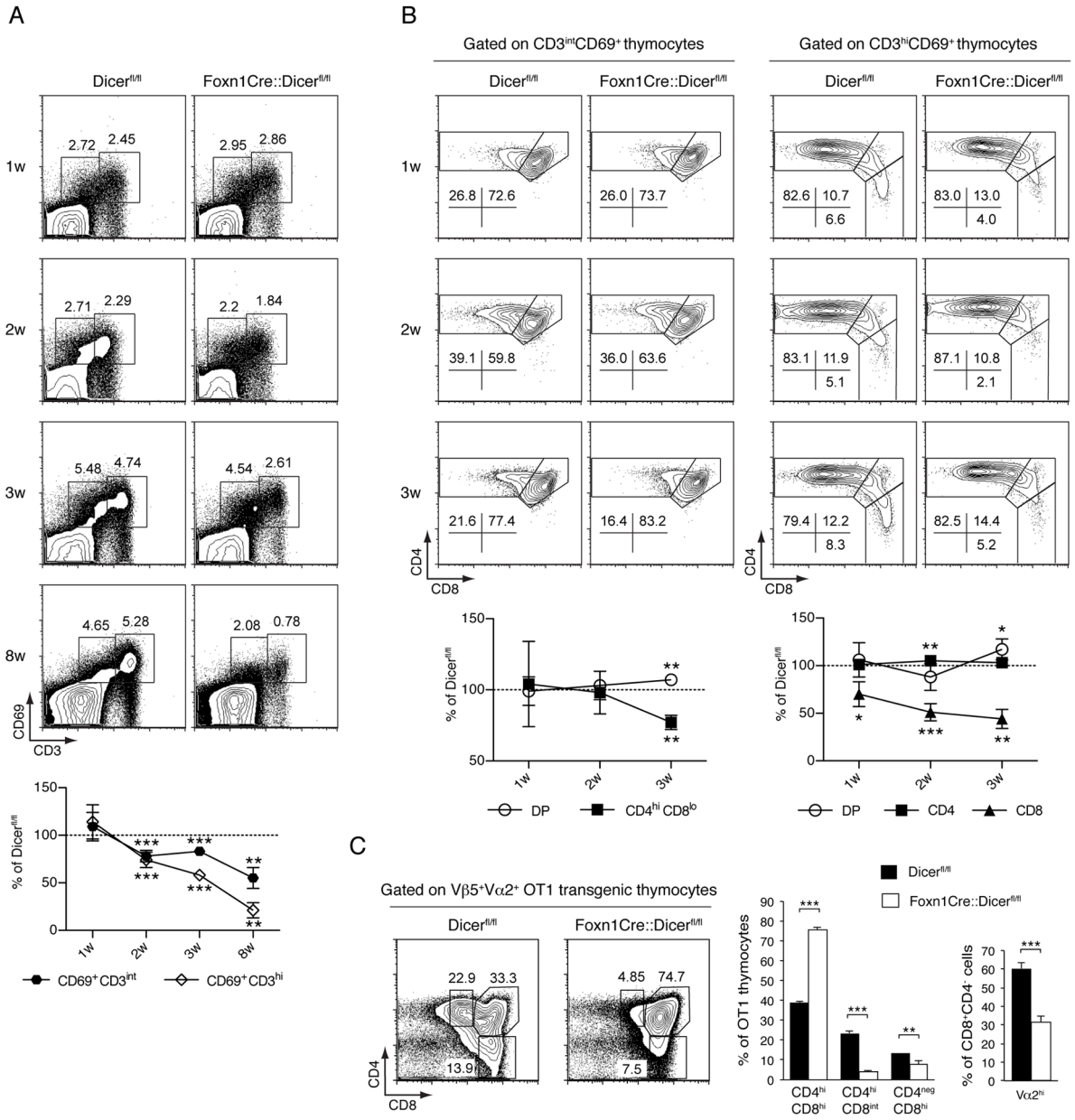

FIGURE 4.

Dicer expression in TECs is required for efficient thymocyte positive selection.(A) Upper panels: Flow cytometric analysis was performed on all thymocytes excluding double negative cells isolated from Dicer$^{fl/fl}$ and Foxn1-Cre::Dicer$^{fl/fl}$ mice of indicated ages. Representative plots of CD69 and CD3 expression analyses of total thymocytes are shown. Lower graph: Changes in the relative frequency of CD69^{+}CD3^{int} and CD69^{+}CD3^{hi} thymocytes over time in Foxn1-Cre::Dicer$^{fl/fl}$ mice in comparison to Dicer$^{fl/fl}$ animals; ** indicates $p<0.01$; *** $p<0.001$. Data are representative of at least two separate experiments with three mice per group. (B) Representative plots of CD4 and CD8 expression analyses of CD69^{+}CD3^{int} (upper left panels) and CD69^{+}CD3^{hi} thymocytes (upper right panels). Lower left graph: Kinetic changes in the relative frequency of the DP and CD4^{+}CD8^{int} phenotypes among CD69^{+}CD3^{int} thymocytes in Foxn1-Cre::Dicer$^{fl/fl}$ mice when compared to Dicer$^{fl/fl}$ animals. Lower right graph: Kinetic changes in the relative frequency of the DP, SP CD4

and SP CD8 phenotypes among $CD69^{+}CD3^{hi}$ thymocytes in Foxn1-Cre::$Dicer^{fl/fl}$ mice when compared to $Dicer^{fl/fl}$ animals. The data in the lower graphs shows the mean ± SD; *denotes $p<0.05$; ** $p<0.01$; *** $p<0.001$. The results are representative of 2 independent experiments with at least 3 mice per group. (C) Flow cytometric analysis of 4 week old $Dicer^{fl/fl}$ and Foxn1-Cre::$Dicer^{fl/fl}$ mice reconstituted at birth with OT-1 TCR transgenic fetal liver cells. Left panels: CD4 and CD8 expression on OT1 TCR transgenic thymocytes. The dot blot graphs are representative of at least three independent experiments. The bar graphs demonstrate the relative frequency of OT1 TCR transgenic $CD4^{hi}CD8^{hi}$, $CD4^{hi}CD8^{int}$ and $CD4^{-}CD8^{hi}$ cells in each gate of left panels (left graph) and the relative frequency of $CD4^{-}CD8^{hi}$ thymocytes expressing high $V\alpha2^{+}$ cell surface amounts as an indicator of thymocyte positive selection (right graph). Black bars: $Dicer^{fl/fl}$ mice; white bars: Foxn1-Cre::$Dicer^{fl/fl}$ mice. The values represent mean ±SD with at least 3 mice per group; ** denotes $p<0.01$; *** $p<0.001$. Data are representative of at least 2 separate experiments with each three or more mice per group.

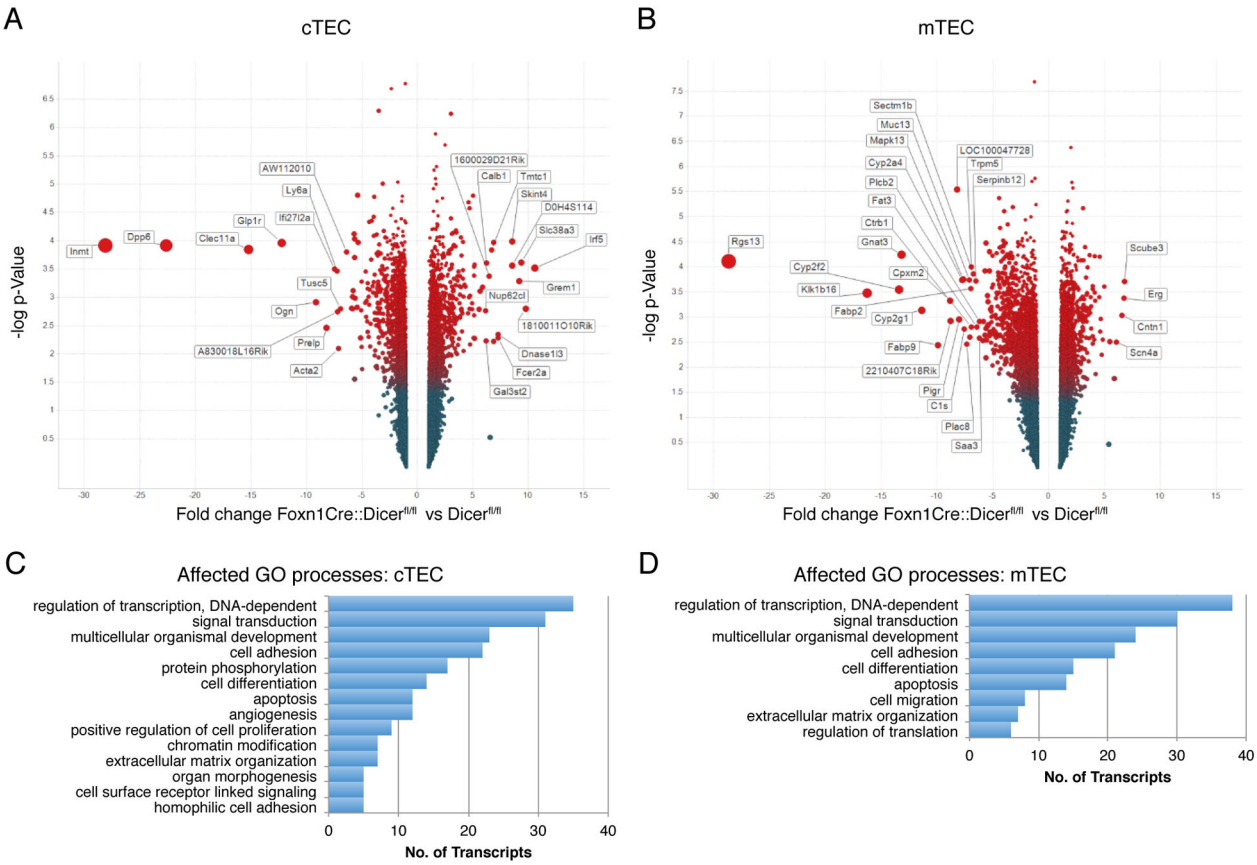

FIGURE 5.

Analysis of gene expression changes in Dicer-deficient TEC and its impact on cell signaling. Volcano plot analysis of mRNA expression changes in cTEC (A) and mTEC (B) from two week old Foxn1-Cre::Dicer$^{fl/fl}$ mice compared to Dicer$^{fl/fl}$ mice. Positive values on the X-axis indicate an up-regulation of transcripts in mutant TEC presented as fold changes, whereas negative values specify down-regulated transcripts shown as fold changes. The Y-axis represents a log scale revealing the corrected p-value for a two-way analysis of variance of the differences between samples. The data represents two separate biological replicates with at least 10 mice per group. The bar graphs show gene ontology pathways significantly affected (corrected $p<0.05$) in cTEC(C) and mTEC (D), respectively.

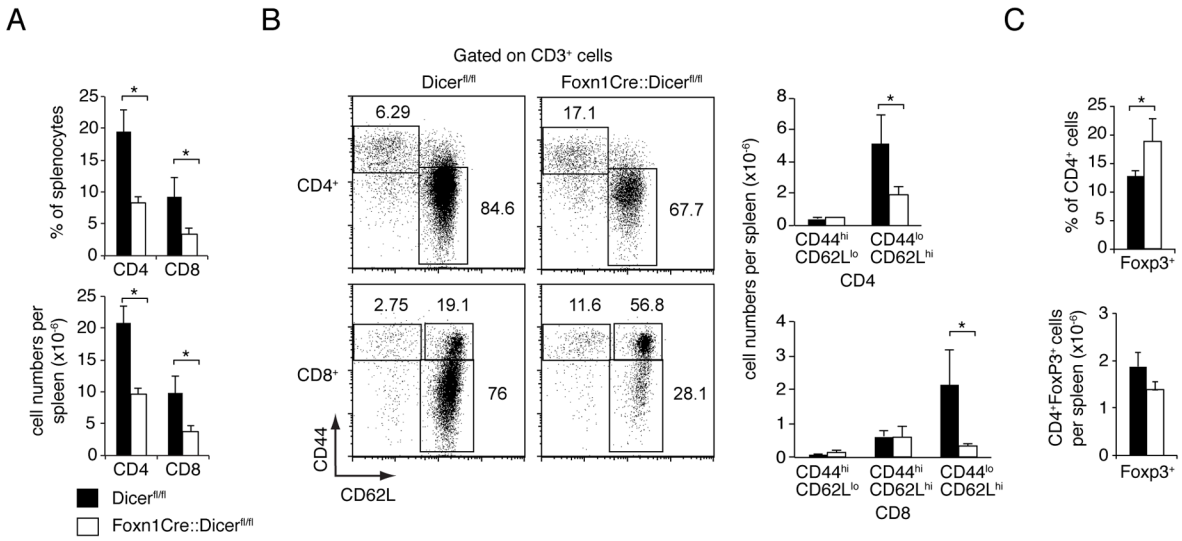

FIGURE 6.

Dicer deficiency in TECs results in altered T cell numbers. (A) Relative frequencies and absolute cell numbers (mean ± SD) of splenic CD4 and CD8 T cells in 8 week old Dicer$^{fl/fl}$ (black bars) and Foxn1-Cre::Dicer$^{fl/fl}$mice (white bars); * indicates $p<0.05$. Data are representative of three separate experiments with at least 3 mice per group. (B) Left panels: Representative analysis of CD44 and CD62L expression among splenic T cells from 8 week old Dicer$^{fl/fl}$ and Foxn1-Cre::Dicer$^{fl/fl}$mice. The numbers show the relative frequency of a given subpopulation as identified by the drawn gate. Right graphs: Absolute numbers (mean ± SD) of T cells from 8 week old Dicer$^{fl/fl}$(black bars) and Foxn1- Cre::Dicer$^{fl/fl}$mice (white bars) with naïve and memory phenotypes; * indicates $p<0.05$. Data are representative of three separate experiments with at least 3 mice per group. (C) Relative frequency (upper graph) and absolute cell numbers (lower graph) of splenic CD4+Foxp3+ T cells in 8 week old Dicer$^{fl/fl}$(black bars) and Foxn1-Cre::Dicer$^{fl/fl}$mice (white bars); * indicates $p<0.05$. Data are representative of two separate experiments with at least 3 mice per group.

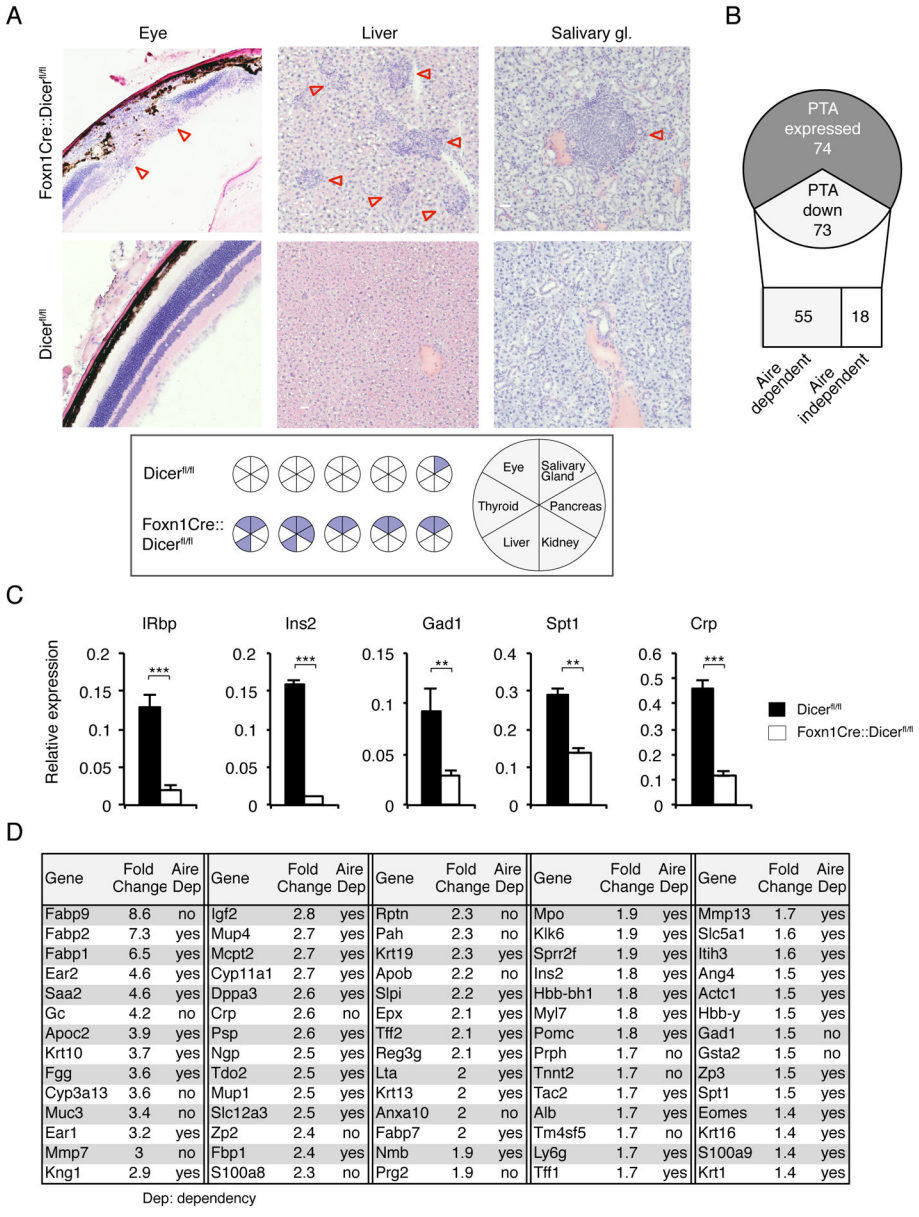

D

Gene	Fold Change	Aire Dep	Gene	Fold Change	Aire Dep	Gene	Fold Change	Aire Dep	Gene	Fold Change	Aire Dep	Gene	Fold Change	Aire Dep
Fabp9	8.6	no	Igf2	2.8	yes	Rptn	2.3	no	Mpo	1.9	yes	Mmp13	1.7	yes
Fabp2	7.3	yes	Mup4	2.7	yes	Pah	2.3	no	Klk6	1.9	yes	Slc5a1	1.6	yes
Fabp1	6.5	yes	Mcpt2	2.7	yes	Krt19	2.3	yes	Sprr2f	1.9	yes	Itih3	1.6	yes
Ear2	4.6	yes	Cyp11a1	2.7	yes	Apob	2.2	no	Ins2	1.8	yes	Ang4	1.5	yes
Saa2	4.6	yes	Dppa3	2.6	yes	Slpi	2.2	yes	Hbb-bh1	1.8	yes	Actc1	1.5	yes
Gc	4.2	no	Crp	2.6	no	Epx	2.1	yes	Myl7	1.8	yes	Hbb-y	1.5	yes
Apoc2	3.9	yes	Psp	2.6	yes	Tff2	2.1	yes	Pomc	1.8	yes	Gad1	1.5	no
Krt10	3.7	yes	Ngp	2.5	yes	Reg3g	2.1	yes	Prph	1.7	no	Gsta2	1.5	no
Fgg	3.6	yes	Tdo2	2.5	yes	Lta	2	yes	Tnnt2	1.7	no	Zp3	1.5	yes
Cyp3a13	3.6	no	Mup1	2.5	yes	Krt13	2	yes	Tac2	1.7	yes	Spt1	1.5	yes
Muc3	3.4	no	Slc12a3	2.5	yes	Anxa10	2	no	Alb	1.7	yes	Eomes	1.4	yes
Ear1	3.2	yes	Zp2	2.4	no	Fabp7	2	yes	Tm4sf5	1.7	no	Krt16	1.4	yes
Mmp7	3	no	Fbp1	2.4	yes	Nmb	1.9	yes	Ly6g	1.7	yes	S100a9	1.4	yes
Kng1	2.9	yes	S100a8	2.3	no	Prg2	1.9	no	Tff1	1.7	yes	Krt1	1.4	yes

Dep: dependency

FIGURE 7.

Autoimmunity in aged Foxn1-Cre::Dicer$^{fl/fl}$ mice.(A) Upper panels: H&E staining of eye, liver and salivary gland tissue from 32 week old female Dicer$^{fl/fl}$ and Foxn1-Cre::Dicer$^{fl/fl}$ mice that had been T cell depleted at 2 weeks of age and allowed to autologously reconstitute their T cell compartment. Lower panel: Graphic summary of organ infiltrations in 32 week old Dicer$^{fl/fl}$ and Foxn1-Cre::Dicer$^{fl/fl}$ mice following transient T cell depletion at 2 weeks of age (each circle represents an individual mouse). Data is representative of two independent experiments with each 5 mice per group. (B) Graphic representation of changes in microarray measured expression of 147 Aire-dependent and Aire-independent peripheral tissue antigens (PTA) in purified mTEC from two week old Foxn1-Cre::Dicer$^{fl/fl}$ and Dicer$^{fl/fl}$ mice. (C) RT-PCR analysis for the expression of retinal (IRbp), salivary gland (Spt1), hepatic (CRP) and pancreatic (Ins2, Gad1) peripheral tissue antigens in purified

mTEC from 2 week old Dicer$^{fl/fl}$ (black bars) and Foxn1-Cre::Dicer$^{fl/fl}$ mice (white bars). Gapdh was used as a reference for data normalization. The data is representative of 2 separate experiments and indicate the mean ± SD of at least 3 mice per group;** signifies $p<0.01$; *** $p<0.001$.(D) Decreased PTA expression in mTEC as a consequence of Dicer deletion. PTA expression was analyzed in mTEC from 2 week old Foxn1-Cre::Dicer$^{fl/fl}$mice using microarray and compared to the expression profile of age-matched, wild type mTEC.